



Yao, A.M., Keen, S.A.J., Burnham, D.R., Leach, J., Di Leonardo, R., McGloin, D. and Padgett, M.J. (2009) *Underdamped modes in a hydrodynamically coupled microparticle system*. *New Journal of Physics* 11 (2009): 053007

<http://eprints.gla.ac.uk/32796/>

Deposited on: 9th October 2012

Underdamped modes in a hydrodynamically coupled microparticle system

This article has been downloaded from IOPscience. Please scroll down to see the full text article.

2009 New J. Phys. 11 053007

(<http://iopscience.iop.org/1367-2630/11/5/053007>)

View [the table of contents for this issue](#), or go to the [journal homepage](#) for more

Download details:

IP Address: 130.209.6.42

The article was downloaded on 09/10/2012 at 16:08

Please note that [terms and conditions apply](#).

Underdamped modes in a hydrodynamically coupled microparticle system

A M Yao^{1,5}, S A J Keen¹, D R Burnham^{2,3}, J Leach¹,
R Di Leonardo⁴, D McGloin³ and M J Padgett¹

¹ SUPA, Department of Physics and Astronomy, University of Glasgow,
Glasgow, UK

² SUPA, School of Physics and Astronomy, University of St Andrews,
St Andrews, UK

³ Electronic Engineering and Physics Division, University of Dundee,
Nethergate, Dundee, UK

⁴ CNR-INFM, CRS SOFT c/o Dipartimento di Fisica, Università di Roma
La Sapienza, I-00185, Roma, Italy

E-mail: a.yao@physics.gla.ac.uk

New Journal of Physics **11** (2009) 053007 (8pp)

Received 8 December 2008

Published 19 May 2009

Online at <http://www.njp.org/>

doi:10.1088/1367-2630/11/5/053007

Abstract. When micron-sized particles are trapped in a linear periodic array, for example, by using optical tweezers, they interact only through the hydrodynamic forces between them. This couples the motion of the spheres and it has been predicted that an extended system might behave as an elastic medium that could support underdamped propagating waves. In practice, these underdamped modes can be observed only with massive particles in very stiff traps and very low viscosity fluids. We have been able to realize these conditions by trapping water droplets in air. Even with a system of just two particles we were able to observe the coupled oscillatory motion predicted: underdamping of the symmetric (collective) mode and overdamping of the asymmetric (relative) mode.

⁵ Author to whom any correspondence should be addressed.

Contents

1. Introduction	2
2. Dynamics of optically trapped microparticles	3
3. Experimental configuration	4
4. Results and analysis	6
5. Conclusion	7
Acknowledgments	8
References	8

1. Introduction

Optically trapped microparticles are becoming an increasingly useful tool in the study of hydrodynamic interactions in colloidal suspensions [1]–[3]. Optical tweezers allow a micron-sized particle to be localized, or trapped, near the focus of a beam. Using holographic optical tweezers, many foci can be created simultaneously and thus many particles can be accurately positioned to form a periodic structure. While the mean position of each particle is fixed by its trap, fluctuating thermal forces cause small displacements away from the trap centre. These thermal forces acting on a particle cause fluid motion around it which in turn affects the velocity of the other particles. This is known as hydrodynamic interaction.

It has been shown [1]–[3] that microparticles localized in optical traps in this way form a hydrodynamically coupled array, whose behaviour is quantitatively explained by a model based on the Oseen superposition approximation. The Oseen tensor relates the velocities of individual particles to the forces acting on the system and can be decomposed into components that describe motion either along the line of the centres (longitudinal) or perpendicular to it (transverse). These components couple the fluctuations so that the particle co-ordinates are no longer independent, resulting in different *modes* of propagation. Recently, Polin *et al* [2] predicted that trapping large spheres strongly in a low-viscosity medium would show the crossover from overdamped dynamics to a regime of underdamped propagating elastic waves with uniformly negative group velocities (see figure 3 of [2]).

Until recently, standard methods of digital video analysis [4]–[6] have only allowed particles to be tracked at tens of Hz, typically writing images to a buffer before downloading onto a computer. As a result, most authors were limited to trapping particles in a relatively viscous medium, such as a water–glycerol mixture, in order to slow down the particle dynamics to a timescale accessible to a conventional video camera. Recent advances in camera technology have meant that high-speed cameras can now be used to track many particles simultaneously at frame rates of kHz for indefinite periods of time [3, 7, 8] thus allowing analysis of particles trapped in much less viscous media, such as air. The lower damping means that trapping particles in air is significantly more difficult [9] and it is only recently that this has been extended to the holographic trapping of multiple particles [10].

We use a CMOS camera with a hardware implementation of centre of mass tracking [11] to carefully track the positions of two water droplets trapped in air, which is ~ 50 times less viscous than water. Using the Oseen superposition approximation, we calculate and analyse the longitudinal and transverse modes of the system. We demonstrate experimental verification of

the crossover to underdamped motion predicted by Polin *et al* and confirm the mode-dependent modification of the damping force due to hydrodynamic coupling.

2. Dynamics of optically trapped microparticles

The motion of a single spherical microparticle in an optical trap with harmonic trapping potential is described by the Einstein–Ornstein–Uhlenbeck theory of Brownian motion [12]:

$$m\ddot{\mathbf{r}}(t) + \gamma_0\dot{\mathbf{r}}(t) + \kappa\mathbf{r}(t) = \mathbf{F}^B(t), \quad (1)$$

where $\mathbf{r}(t)$ is the trajectory of a particle of mass m and radius a localized in a trap of strength κ and $\gamma_0 = 6\pi\eta a$ is its viscous drag coefficient in a fluid of viscosity η . $\mathbf{F}^B(t)$ describes the stochastic forces that arise from the thermal fluctuations in the fluid. These give rise to Brownian motion and are Gaussian random variables with

$$\langle F^B(t) \rangle = 0 \quad \text{and} \quad \langle F^B(t)F^B(t') \rangle = 2k_B T \gamma_0 \delta(t - t'). \quad (2)$$

When more than one particle is present, the motion of any given particle will be influenced by the configuration and motion of the other particles. These hydrodynamic interactions between the particles tend to favour correlated motion, where every particle can move within the ‘slip-stream’ of its neighbours, and hinder anti-correlated motion, where particles move in opposite directions [13]. The effect of the hydrodynamic interaction, then, is to modify the damping force acting on the particles. For a two-dimensional array of particles \mathbf{R} at locations \mathbf{r}_i^α ($i = 1, \dots, N, \alpha = 1, 2$) the equation of motion in the presence of an external force \mathbf{F}^H becomes $\dot{\mathbf{R}}(t) = \mathbf{H}(\mathbf{R}) \cdot \mathbf{F}^H$. $\mathbf{H}(\mathbf{R})$ is the N -body Oseen tensor, which describes particle i ’s motion in the α direction due to a force applied to particle j in the β direction. In the limit of large interparticle separation it can be approximated by [14]:

$$H_{ij}^{\alpha\beta} = \frac{1}{\gamma_0} \delta_{\alpha\beta} \delta_{ij} + \frac{3}{4\gamma_0} \frac{a}{r_{ij}} (1 - \delta_{ij}) \left(\delta_{\alpha\beta} + \frac{r_{ij}^\alpha r_{ij}^\beta}{r_{ij}^2} \right), \quad (3)$$

where $r_{ij}^{\alpha,\beta} = r_i^{\alpha,\beta} - r_j^{\alpha,\beta}$ is the particle separation in the α, β direction, r_{ij} is the distance between the particles and we have assumed that all the particles have radius a .

We introduce the equilibrium positions, or trap centres, $\mathbf{R}^0 = \{\mathbf{r}_i^0\}$, and assume that the spheres fluctuate about their equilibrium positions are small with respect to interparticle distances so that we can replace $\mathbf{H}(\mathbf{R})$ with $\mathbf{H}^0 = \mathbf{H}(\mathbf{R}^0)$. A hydrodynamically coupled array of microparticles positioned in optical traps of equal strength, then, forms a thermally excited, viscously damped, dynamical system whose behaviour is quantitatively explained by a Langevin model based on the Oseen superposition approximation:

$$m\ddot{\mathbf{r}}_i(t) + \sum_j^N (\mathbf{H}^{-1})_{ij} \cdot \dot{\mathbf{r}}_j(t) + \kappa(\mathbf{r}_i(t) - \mathbf{r}_i^0) = \mathbf{F}_i^B(t), \quad (4)$$

where $\mathbf{F}_i^B(t)$ describes the thermal force acting on the i th particle. The motion of the particles can be analysed in terms of the predicted eigenmodes for hydrodynamically coupled spheres [15], which are eigenvectors of the Oseen tensor, \mathbf{H}^0 . The time evolution of any mode, ξ_j , in a particular polarization (parallel or perpendicular to the array’s axis) can then be described

by the N -body Langevin equation:

$$m\ddot{\xi}_j + \frac{\gamma_0}{\lambda_j} \dot{\xi}_j + \kappa \xi_j = f_j^B(t), \quad (5)$$

where λ_j is the eigenvalue associated with the mode ξ_j and the thermal fluctuations $f_j^B(t)$ are influenced by hydrodynamic interactions so that

$$\langle f_j^B(t) f_j^B(t') \rangle = \frac{2k_B T \gamma_0}{\lambda_j} \delta(t - t'). \quad (6)$$

Comparing (5) with (1), it is clear that the effect of the hydrodynamic interaction is to modify the damping force, γ_0 , by an amount dependent on the eigenvalue of a particular mode of oscillation, λ_j . Collective modes, that is modes in which the particles all move in the same direction, have larger eigenvalues and so experience less damping force, while the opposite is true for relative modes.

Clearly (5) has the form of a damped, driven harmonic oscillator whose general solution is a sum of a transient (the solution for the undriven harmonic oscillator) that depends on initial conditions and is independent of the driving (Brownian) force and a steady-state that is independent of initial conditions and depends on the Brownian force, restoring force and damping force. Each mode is characterized by a complex frequency ω_j given by

$$\omega_j = \frac{i\Gamma_j}{2} \pm \sqrt{\Omega^2 - \left(\frac{\Gamma_j}{2}\right)^2}, \quad (7)$$

where $\Gamma_j = \gamma_0/(m\lambda_j)$ and $\Omega^2 = \kappa/m$. We can then see that there are three distinct regimes in which the behaviour depends on the ratio of Ω and Γ_j : (i) if $\Gamma_j > 2\Omega$ the system is overdamped, (ii) if $\Gamma_j = 2\Omega$ the system is critically damped and (iii) if $\Gamma_j < 2\Omega$ the system is underdamped. Since Γ_j depends on the eigenvalue of a particular mode, λ_j , modes with larger eigenvalues are more likely to be underdamped. This demonstrates how the crossover from overdamping to underdamping is governed by the hydrodynamic coupling. In particular, for the system to be underdamped we require that $\Gamma_j^2/(4\Omega^2) < 1$. Rewriting this as $9(\pi\eta a)^2/(m\kappa\lambda_j^2) < 1$, we see that we can move towards under-damping by decreasing the viscosity of the fluid and/or increasing the mass of the particle, the trap strength and the eigenvalue.

3. Experimental configuration

The experimental configuration is shown in figure 1. A 532 nm Gaussian beam from a Laser Quantum Finesse 4W cw laser is expanded to fill a Holoeye LCR-2500 spatial light modulator (SLM) and is then demagnified via two 4f imaging systems to slightly overfill the back aperture of a Nikon Plan 100 \times (NA = 1.25) oil immersion microscope objective lens and focused through a type one coverslip. The SLM displays an appropriate hologram to create two optical traps, each of power 300–400 mW, separated by a few microns. The power input to the experiment is controlled by a half wave plate and polarizing beam cube with a second wave plate controlling the polarization incident on the SLM to optimize efficiency. The sample is illuminated with a long working distance (LWD) Mitutoyo 100 \times (NA = 0.55) microscope objective lens via Köhler illumination (not shown) from a halogen fibre illuminator (ThorLabs). The Nikon objective images the sample, via an appropriate tube lens, onto the CMOS camera. The integration of the centre-of-mass processing means that it is only the particle positions

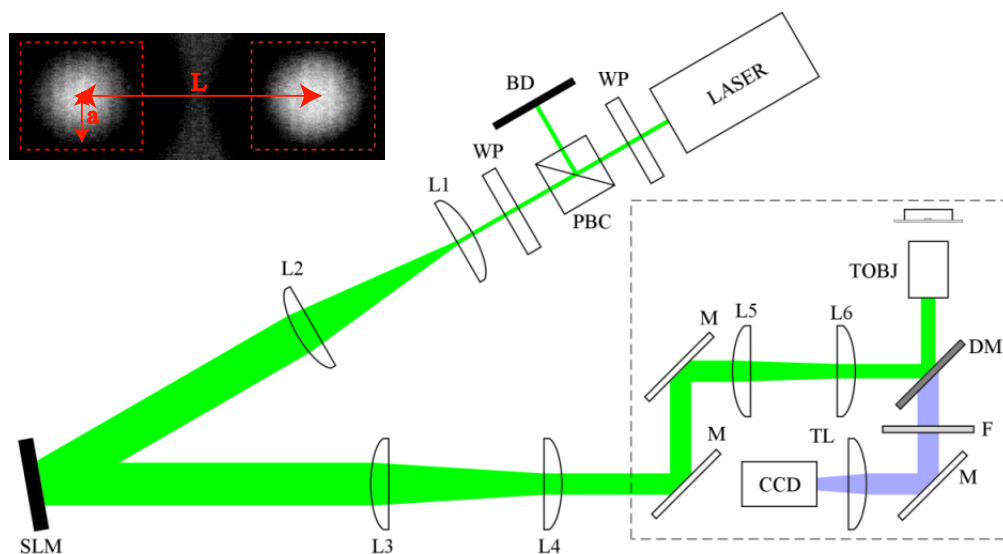


Figure 1. Holographic optical tweezing apparatus. A Gaussian beam with power controlled by half wave plate and polarizing beam cube is expanded with lenses L1 and L2 to fill the Holoeye LCR-2500 SLM. The SLM efficiency is optimized with rotation of incident polarization by the second half wave plate. The reflected beam is demagnified using lenses L3 to L6 in two 4f imaging systems and steered by mirrors M and DM to slightly overfill the back aperture of a Nikon objective (TOBJ). The sample is illuminated with Köhler illumination (not shown). The Nikon objective with appropriate tube lens (TL) images the sample through a dichroic mirror (DM) and filter (F) onto the CMOS camera (CMOS). The apparatus within the dashed box is mounted perpendicular to the optical bench such that the tweezer propagates against gravity.

rather than the whole image that are transferred to the computer, which allows indefinite monitoring of up to 16 particles at several kHz without data management problems. In this case, we monitor at around 3.5 kHz.

To form the droplets, we nebulize a salt solution ($20\text{--}80\text{ g l}^{-1}$) with an Omron MicroAir NE-U22 nebulizer to produce polydisperse liquid droplets with a mass median aerodynamic diameter (MMAD), of $4.9\ \mu\text{m}$. Adding impurities to pure water droplets allows them to reach equilibrium with their surrounding environment at larger sizes [16]. As we wish to observe underdamped motion, it is desirable to trap particles with as large a mass as possible so a high concentration of salt is used to maximize the radii of the particles. The size of the ‘captured’ droplets is also linearly dependent on the trapping power [10] so here we use as high a laser power as possible while still allowing the ‘capture’ of droplets to be frequent. A problem in quantitative analysis is the difficulty in accurately sizing water droplets from video images alone, due not only to their dynamic nature but also to the poor definition of their edges on the video output.

The sample chamber is a plastic enclosure $\simeq 9\text{ mm}$ high and $\simeq 35\text{ mm}$ in diameter with a type zero coverslip on top and a type one coverslip on the bottom. A heavy ring of metal is placed on top to prevent movement of the coverslip with sample stage movement. At the top of the chamber we place tissue paper saturated in distilled water to assist in creating a

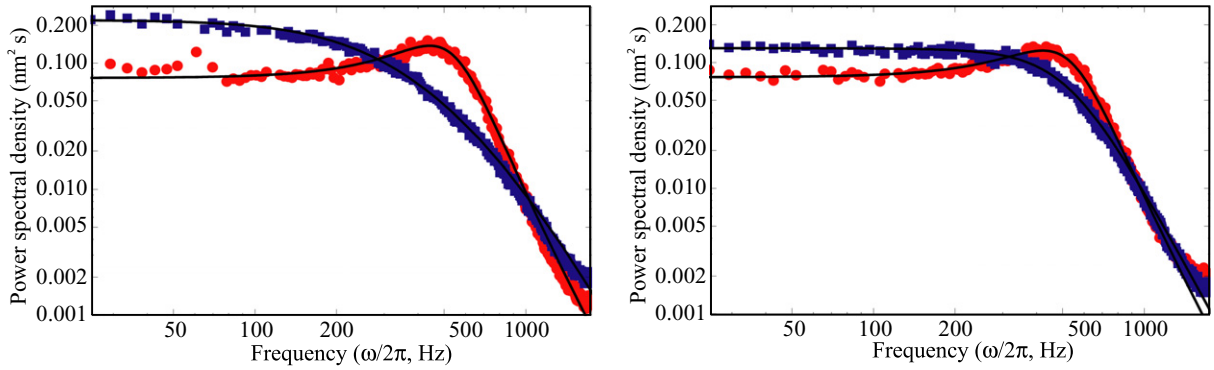


Figure 2. Power spectral densities for parallel (left) and perpendicular (right) modes of two trapped water droplets. Circles (red) show the under-damped, collective mode, squares (blue) show the over-damped, relative mode. Solid lines show the Lorentzian fits.

humid environment. The lower coverslip was treated with Decon 90 to increase hydrophilicity so that settling aerosol produces a thin uniform water layer beneath the trapping region, thereby minimizing aberration of the focused spot. To control the droplet-to-water surface height, the sample is placed on a three axis translation stage that moves around the fixed Nikon objective. The axial translation was manually adjusted. We first focus the beam $\simeq 15 \mu\text{m}$ above the coverslip for ease of trapping; once caught the droplet is moved away from the water surface.

4. Results and analysis

From the measured x, y positions we calculate the power spectra of the modes. For a one-dimensional chain of particles, the modes are eigenvectors of the matrices [2]:

$$(\gamma_0 H)_{ij}^{\parallel} = \begin{cases} 1, & i = j, \\ 3a/(2r_{ij}), & i \neq j, \end{cases} \quad \text{and} \quad (\gamma_0 H)_{ij}^{\perp} = \begin{cases} 1, & i = j, \\ 3a/(4r_{ij}), & i \neq j. \end{cases} \quad (8)$$

Thus for two particles, the normal modes are: $(x_1 \pm x_2)/\sqrt{2}$ and $(y_1 \pm y_2)/\sqrt{2}$ with eigenvalues $\lambda_{\pm}^{\parallel} = 1 \pm 3a/(2L)$ and $\lambda_{\pm}^{\perp} = 1 \pm 3a/(4L)$, respectively. Note, x and y correspond to movement parallel and perpendicular to the line of particles and L is the distance between them, which in this case is $\approx 15 \mu\text{m}$.

We assume that the stochastic force due to thermal agitation, f_j^B , has a white noise power spectrum

$$S^B(\omega) = \frac{\Gamma_j k_B T}{\pi}. \quad (9)$$

Then Fourier transforming (5) and using (9) we obtain the power spectrum of mode fluctuations:

$$S^{\xi}(\omega) = \frac{k_B T}{\pi \kappa} \frac{\Omega^2 \Gamma_j}{(\Omega^2 - \omega^2)^2 + \omega^2 \Gamma_j^2}. \quad (10)$$

The power spectra for the modes are shown in figure 2. In both cases it is clear how the particle dynamics changes from an overdamped Lorentzian spectrum for the relative mode (blue squares) to an underdamped spectrum for the collective mode (red circles) with a faster roll-off

and the appearance of a resonance peak at $\omega = \sqrt{\Omega^2 - \Gamma_j^2}/2$. We note that this frequency is lower than that for a damped but undriven oscillator; a familiar component of the theory of forced simple harmonic motion [17]. In addition, we see a bigger difference in the behaviour of the parallel modes than in the perpendicular modes, which is as we would expect given the difference in the ‘splitting’ of the eigenvalues for the parallel and perpendicular motion.

By fitting these results to (10) we can calculate the trap frequency, Ω , and the damping coefficients Γ_j for each mode.

We find an average trap frequency of $\Omega \simeq 3380 \text{ rad s}^{-1}$, corresponding to a trap strength of $\kappa \simeq 5.98 \text{ pN } \mu\text{m}^{-1}$.

We can calculate the ratio of the eigenvalues from the ratio of the damping coefficients:

$$\begin{aligned}\Lambda^{\parallel} &= \left(\frac{\Gamma_+}{\Gamma_-}\right)^{\parallel} = \left(\frac{\lambda_-}{\lambda_+}\right)^{\parallel} = \frac{1 - (3a/2L)}{1 + (3a/2L)}, \\ \Lambda^{\perp} &= \left(\frac{\Gamma_+}{\Gamma_-}\right)^{\perp} = \left(\frac{\lambda_-}{\lambda_+}\right)^{\perp} = \frac{1 - (3a/4L)}{1 + (3a/4L)}.\end{aligned}\quad (11)$$

We find $\Lambda^{\parallel} = 0.34$ and $\Lambda^{\perp} = 0.60$, which agree very well with the predicted values of 0.33 and 0.60, respectively, calculated using the eigenvalues and an estimated particle radius, a , of $\approx 5.0 \mu\text{m}$ and separation, L , of $15.05 \mu\text{m}$.

As mentioned earlier, it can be difficult to accurately size water droplets from video images. Note, however, that (11) also allows us to calculate the size of the particles from the experimental results, assuming that both particles are of the same size. Rearranging, we find

$$a = \frac{2L}{3} \left(\frac{1 - \Lambda^{\parallel}}{1 + \Lambda^{\parallel}}\right) = \frac{4L}{3} \left(\frac{1 - \Lambda^{\perp}}{1 + \Lambda^{\perp}}\right).\quad (12)$$

Using this we calculate the radius of the particles, a , to be $4.93 \mu\text{m}$, which is very close to the estimated value of $\approx 5.0 \mu\text{m}$. Using this value of a in the calculation for Λ^{\parallel} and Λ^{\perp} gives values of 0.341 and 0.605, respectively.

In addition to the particle size, the damping coefficients also allow us to calculate the viscosity of the fluid, since $\Gamma_j = \gamma_0/(m\lambda_j) = 6\pi\eta a/(m\lambda_j)$. In this case, we calculate the average viscosity, η , to be $2.0 \times 10^{-5} \text{ kg (m s)}^{-1}$ which is in reasonable agreement with the expected value of $1.86 \times 10^{-5} \text{ kg (m s)}^{-1}$ for air at room temperature (25°C).

The effect of underdamping is to introduce a real part to the radical so that the general solution for the mode now consists of a periodic oscillation with decaying amplitude. This is clearly seen in the autocorrelation plots shown in figure 3. The solid (red) lines corresponding to the collective mode in parallel and perpendicular planes are oscillatory, as would be expected for an underdamped mode. In contrast, the dashed (blue) lines, corresponding to the anti-correlated, over-damped modes show a simple exponential decay.

5. Conclusion

In conclusion, we have used holographic optical tweezers to trap two water droplets in air. By carefully tracking the positions of the trapped droplets and using the Oseen superposition approximation we were able to calculate and analyse the longitudinal and transverse modes of the system. This allowed us to verify experimentally the transition from overdamped to underdamped modes and show that this is due to hydrodynamical interaction between the particles.

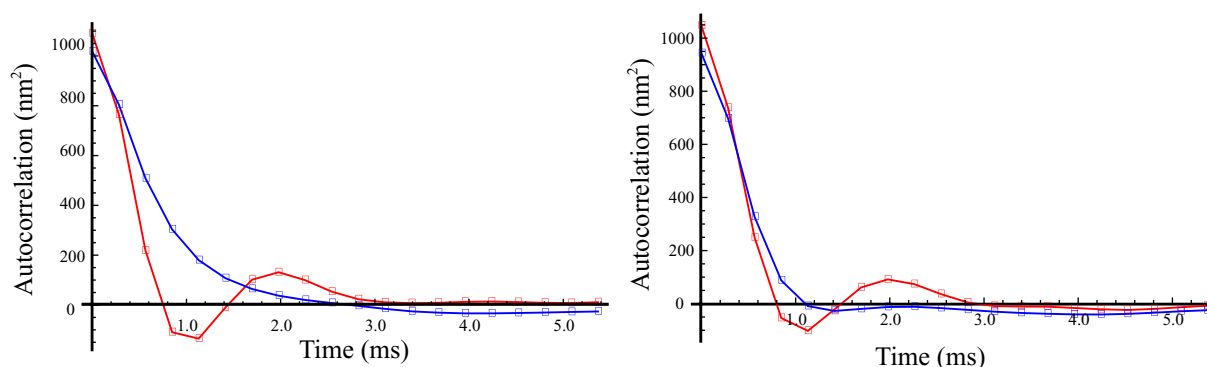


Figure 3. Auto-correlation curves for parallel (left) and perpendicular (right) modes of two trapped water droplets. Red lines correspond to the under-damped, collective mode, blue lines are the over-damped, relative mode.

We expect that extension to systems with a larger number of particles would result in propagating elastic waves with anomalous dispersion and negative group velocities, as predicted by Polin *et al* [2]. However, experimentally this is hampered by the difficulty both in trapping many water droplets in sufficiently strong traps and ensuring that the droplets are of the same size.

Acknowledgments

We thank EPSRC and BBSRC for their support and Stephen M Barnett for very useful discussions. DM is supported by a Royal Society University Research Fellowship.

References

- [1] Meiners J-C and Quake S R 1999 *Phys. Rev. Lett.* **82** 2211–4
- [2] Polin M, Grier D G and Quake S R 2006 *Phys. Rev. Lett.* **96** 088101
- [3] Di Leonardo R, Keen S, Ianni F, Leach J, Padgett M J and Ruocco G 2008 *Phys. Rev. E* **78** 031406
- [4] Crocker J C and Grier D G 1996 *J. Colloid Interface Sci.* **179** 298
- [5] Carter B C, Shubeita G T and Gross S P 2005 *Phys. Biol.* **2** 60–72
- [6] Savin T and Doyle P S 2005 *Biophys. J.* **88** 623–38
- [7] Di Leonardo R, Ruocco G, Leach J, Padgett M J, Wright A J, Girkin J M, Burnham D R and McGloin D 2007 *Phys. Rev. Lett.* **99** 010601
- [8] Gibson G M, Leach J, Keen S, Wright A J and Padgett M J 2008 *Opt. Express* **16** 14561–70
- [9] Omori R, Kobayashi T and Suzuki A 1997 *Opt. Lett.* **22** 816–8
- [10] Burnham D R and McGloin D 2006 *Opt. Express* **14** 4175–81
- [11] Saunter C D, Love G D, Johns M and Holmes J 2005 *Proc. SPIE* **6018** 429–35
- [12] Kubo R, Toda M and Hashitsume N 1985 *Statistical Physics* vol 2 (Heidelberg: Springer)
- [13] Dufresne E R, Squires T M, Brenner M P and Grier D G 2000 *Phys. Rev. Lett.* **85** 3317–20
- [14] Doi M and Edwards S 1986 *The Theory of Polymer Dynamics* (Oxford: Oxford University Press)
- [15] Happel J and Brenner H 1991 *Low Reynolds Number Hydrodynamics* (Dordrecht: Kluwer)
- [16] Monteith J and Unsworth M 2008 *Principles of Environmental Physics* (New York: Academic)
- [17] Fowles G R 1986 *Analytical Mechanics* (Philadelphia: Saunders College Publishing)